

A Double-Transition Scenario for Anomalous Diffusion in Glass-Forming Mixtures

Th. Voigtmann^{1,2} and J. Horbach¹

¹*Institut für Materialphysik im Weltraum, Deutsches Zentrum für Luft- und Raumfahrt (DLR), 51170 Köln, Germany*

²*Zukunftskolleg und Fachbereich Physik, Universität Konstanz, 78457 Konstanz, Germany*

(Dated: September 13, 2009)

We study by molecular dynamics computer simulation a binary soft-sphere mixture that shows a pronounced difference in the species' long-time dynamics. Anomalous, power-law-like diffusion of small particles arises, that can be understood as a precursor of a double-transition scenario, combining a glass transition and a separate small-particle localization transition. Switching off small-particle excluded-volume constraints slows down, rather than enhances, small-particle transport.

PACS numbers: 61.43.-j 64.70.Q- 66.10.-x

Transport properties in disordered media are important in a wide range of applications from biophysics to geosciences. Intriguing behavior arises from 'fast' species moving through a dense host system, such as power-law-like dynamical conductivities of ion-conducting melts [1], and 'anomalous diffusion': mean-squared displacements (MSD) grow like $\delta r^2 \sim t^\mu$ (with some positive $\mu < 1$) over large time windows, instead of obeying Einstein's law for ordinary diffusion ($\mu = 1$). Examples are tracer experiments in cellular environments [2–4], zeolites [5, 6], gels [7, 8], amorphous semi- and photoconductors [9], or confined colloidal suspensions [10–12].

These systems can be thought of as mixtures composed of a small (fast) species and slow (big) host particles providing a complex confining structure (called 'molecular crowding' in biophysical literature). Considering single tracers moving in a random environment [13–15] invokes as a reference point the single-file diffusion of non-overtaking particles, $\delta r^2 \sim t^{1/2}$ [16–18]. Such modeling obviously leaves out two aspects: the dynamics leading to a time-scale separation in the first place, and interactions among the carrier particles.

To highlight the remarkable features arising from dynamical many-body effects in anomalous diffusion, we investigate a binary, disparate-size soft-sphere mixture. We show how anomalous diffusion can be interpreted as a high-density phenomenon, specifically as the approach to a double-glass transition. Many-body interactions manifest themselves in a striking way in the dynamics: *releasing* excluded-volume constraints, the small-particle mobility is *reduced* at long times, rather than enhanced.

The appearance of two kinds of glasses – one where both particle species freeze, one where the smaller one stays mobile – has been predicted [19–21] using mode-coupling theory of the glass transition (MCT) [22], and indicated in colloidal experiments [23, 24] and molecular-dynamics simulations [25]. MCT qualitatively explains fast-ion diffusion in sodium silicate melts [26] as a precursor of this scenario. Two transitions arise that have different microscopic origins: while the slow dynamics of the larger species is dominated by caging on the nearest-neighbor scale, the single-particle dynamics of

the smaller species exhibits a continuously diverging localization length. This latter leads to anomalous diffusion. The same phenomenology holds in MCT when big particles are immobile from the outset [27–29], and in the Lorentz gas [30, 31].

The Lorentz gas (LG) is the exemplary off-lattice model for particle localization: a single classical point particle moves between randomly distributed, fixed hard-sphere obstacles. At a critical obstacle density, the particle undergoes a localization transition understood as a critical dynamic phenomenon [32]. Continuum percolation theory explains a power-law asymptote for the MSD, $\delta r^2 \sim t^{2/z}$, demonstrated in recent extensive simulations [33–35]. The connection of the LG model to anomalous diffusion in binary glass formers is surprisingly subtle, as we shall point out.

We performed molecular-dynamics (MD) simulations of an equimolar binary mixture of purely repulsive soft spheres, with interaction potential $V_{\alpha\beta}(r) = 4\epsilon_{\alpha\beta}[(r/\sigma_{\alpha\beta})^{-12} - (r/\sigma_{\alpha\beta})^{-6}] + \epsilon_{\alpha\beta}$ for $r < r_- = 2^{1/6}\sigma_{\alpha\beta}$ (zero else), $\alpha, \beta \in (l, s)$. Diameters are chosen additively, $\sigma_{\alpha\beta} = (\sigma_{\alpha\alpha} + \sigma_{\beta\beta})/2$, σ_{ll} . The size ratio, $\sigma_{ss}/\sigma_{ll} = 0.35$, is effectively further reduced by choosing nonadditive energetic interactions, $\epsilon_{ll} = \epsilon_{ss} = 1$ but $\epsilon_{sl} = 0.1$. The temperature $k_B T = 2/3$, and all masses are equal, $m_l = m_s = 1$. The smoothed potential $V(r) \times [(r-r_-)^4 / (h+(r-r_-))]^4$ with $h = 0.005\sigma_{ll}$ provides continuity of energy and forces at the cutoff. Newton's equations of motion were integrated for $N_l = N_s = 1000$ particles with the velocity form of the Verlet algorithm (time step $\delta t = 0.005/\sqrt{48}$ in units $t_0 = [m_l\sigma_{ll}^2/\epsilon_{ll}]^{1/2}$). To avoid crystallization, big-particle diameters were sampled equidistantly from the interval $\sigma_{ll} \in [0.85, 1.15]$, retaining $\sigma_{sl} = (1 + \sigma_{ss})/2$. At each number density ρ , four independent runs were performed. Up to $\rho \leq 2.296\sigma_{ll}^{-3}$, the system was fully equilibrated, requiring equilibration runs between 10^6 and 2×10^8 time steps, followed by production runs of the same length. During equilibration, temperature was fixed by periodic coupling to a stochastic heat bath; production runs were done in the microcanonical ensemble. At the highest density $\rho = 4.215\sigma_{ll}^{-3}$, over 10^9 time steps were performed. No

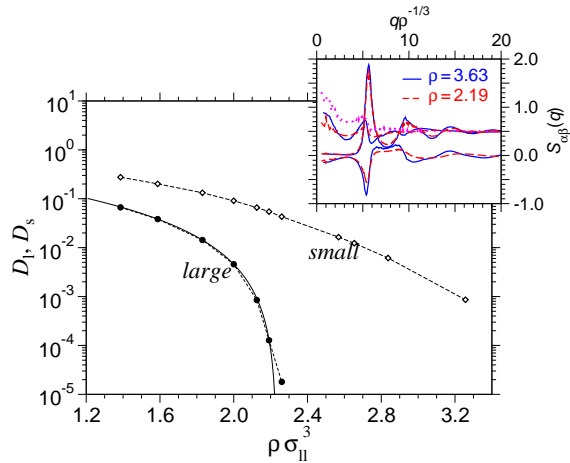


FIG. 1: MD-simulated self-diffusion coefficients for small (D_s) and large particles (D_l) in a disparate-sized binary mixture. The solid line is a power-law fit $\propto (\rho_c - \rho)^\gamma$, where $\rho_c = 2.23$ and $\gamma = 2.1$. Inset: partial static structure factors $S_{\alpha\beta}(q)$ at two different densities, as functions of $q\rho^{-1/3}$. The dotted line is $S_{ss}(q)$ for non-interacting small particles at $\rho = 2.19$.

runs showed signs of demixing or equilibrium phase transitions. We did not find finite-size effects.

Figure 1 displays the self-diffusion constants D_α obtained from the simulated mean-squared displacement (MSD), $\delta r_\alpha^2(t) = \langle (\vec{r}_\alpha^s(t) - \vec{r}_\alpha^s(0))^2 \rangle$ for a singled-out particle at $\vec{r}_\alpha^s(t)$ via $\delta r_\alpha^2(t \rightarrow \infty) \sim 6D_\alpha t$, where possible. A decoupling in the diffusive motion of large and small particles is seen, which becomes more pronounced with increasing density, due to a faster slowing down in D_l than in D_s . At $\rho = 2.296$, D_s is about 2.5 orders of magnitude higher than D_l , and at $\rho \geq 2.568$, big-particle diffusion has ceased over the entire simulation window. Yet, the small-particle MSD still retains a diffusive regime, allowing us to extract $D_s > 0$ up to $\rho = 3.257$. Also shown in Fig. 1 is a fit of D_l by the power law predicted by MCT, $D \sim (\rho_c - \rho)^\gamma$. Fitting yields $\rho_c = 2.23$ and $\gamma = 2.1$. $D_s(\rho)$ allows no convincing similar fit.

The slowing down discussed here is dynamic: no essential changes in the static structure of the system were observed, despite the drastic compression. This is demonstrated by the static structure factors, $S_{\alpha\beta}(q) = \langle \sum_{jk} \exp[-i\vec{q} \cdot (\vec{r}_{\alpha,j} - \vec{r}_{\beta,k})] \rangle$, showing little change with density if plotted as functions of $q^* = q\rho^{-1/3}$ to eliminate a trivial change in length scale (inset of Fig. 1).

The mean-squared displacements are shown in Fig. 2. For the big particles, we observe a standard glass-transition scenario: a two-step process gives rise to a plateau over an increasingly large time window, crossing over to diffusion at increasingly large time, and at a length scale associated with dynamic nearest-neighbor caging, typically around 10% of a particle diameter. Indeed, from the plateau of the $\rho = 2.296$ curve one reads off the cage localization length $r_1^c = \sqrt{\delta r_1^2/6} \approx 0.06 \sigma_{ll}$,

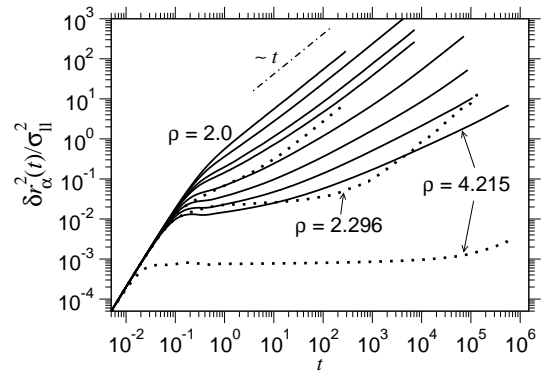


FIG. 2: Mean-squared displacements (MSD), $\delta r_\alpha^2(t)$ for the large (dotted) and small (solid lines) particles in the simulated binary mixture. Densities shown are $\rho\sigma_{ll}^3 = 2.0, 2.296, 4.215$ for $\alpha = l$ and $\rho\sigma_{ll}^3 = 2.0, 2.296, 2.654, 2.837, 3.257, 3.627, 3.906, 4.215$ for $\alpha = s$.

which decreases at larger ρ due to compression. At the same densities, the small-particle MSD behave quite differently, with no sign of two-step glassy dynamics. Instead, they show subdiffusive growth and cross over to ordinary diffusion at increasingly large length and time scales when increasing ρ . This indicates that nearest-neighbour caging is not a dominant mechanism for their slowing down. The subdiffusive regime can be described by power-law variation, $\delta r_s^2(t) \propto t^\mu$ with some $0 < \mu < 1$ that seems to decrease with increasing density.

The small-particle dynamics qualitatively agrees with previous MD results [25], but also with the dynamics found in the Lorentz gas [33–35]. There, subdiffusive growth with apparent density-dependent exponents μ is due to the approach to an asymptotic power law, $\delta r_s^2(t) \sim t^x$, that extends to $t \rightarrow \infty$ at the localization critical point. Careful simulations [33] could establish $x = 2/6.25$ for the LG. To estimate a critical exponent x from Fig. 2 is tempting, but rendered impossible by preasymptotic corrections. It appears that a description of our data using the LG exponent is not convincing.

Our binary mixture differs from the LG *inter alia* through the finite density of interacting small particles. To establish the effect of this distinction, we switch off interactions among small particles, setting $\epsilon_{ss} = 0$ while keeping their number constant. Within simulation accuracy, structure and dynamics of the big particles are unchanged in this ‘transparent-small’ mixture.

Figure 3 compares the small-particle MSD of the two systems. Initially, the transparent small particles show weaker localization, intuitively expected as they have larger free volume available. This trend prevails at low densities. Surprisingly, at high ρ , switching *off* interactions leads to significantly *slower* diffusion compared with the fully interacting case as $t \rightarrow \infty$.

This is emphasized by the lower panel of Fig. 3: the effective exponent $\mu(t) = d[\log \delta r_s^2(t)]/d(\log t)$ crosses over

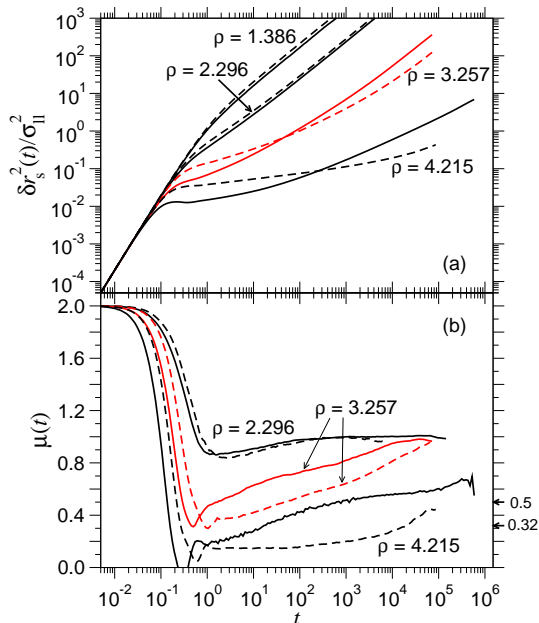


FIG. 3: (a) Small-particle MSD with (solid lines) and without (dashed) interactions among small particles, densities as indicated. (b) Effective exponent $\mu(t) = d[\log \delta r_s^2(t)]/d(\log t)$.

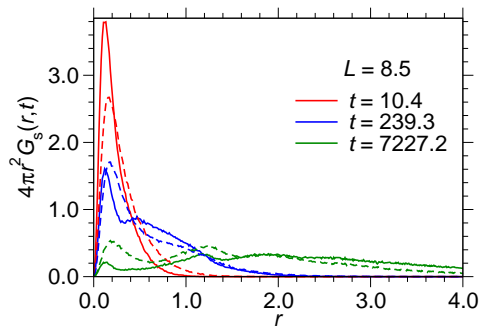


FIG. 4: Self-part of the van Hove correlation function $G_s(r, t)$ for small particles with (solid) and without (dashed lines) mutual interaction, plotted as probability distribution $4\pi r^2 G_s(r, t)$ for times indicated, and at density $\rho = 3.257 \sigma_{II}^{-3}$.

from $\mu(0) = 2$ (ballistic short-time motion) to $\mu(\infty) = 1$ for ordinary diffusion or $\mu(\infty) = 0$ for arrested particles. For the LG model, $\mu(t) \approx x$ for increasingly large time windows close to the localization threshold. No clear plateaus are seen in our data, but switching off small-small interactions at fixed density ρ systematically reduces $\mu(t)$ at long times. For comparison, we have indicated in Fig. 3 the predictions $x = 1/2$ for single-file diffusion and $x = 2/6.25 = 0.32$ from the LG model.

The two reference models suggest a rationale for our finding: removing excluded-volume constraints favors local motion, but in the long run, the exploration of all the cul-de-sacs in the high-density frozen background for the noninteracting small particles becomes vastly less effective than a transport mechanism where inter-

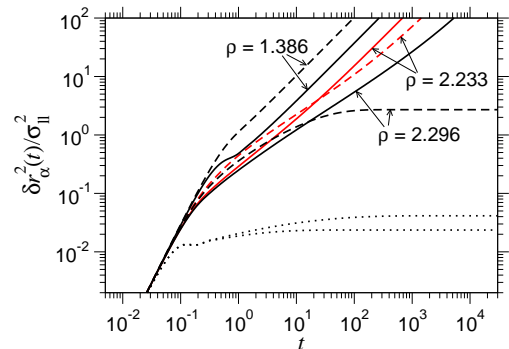


FIG. 5: Mean-squared displacements $\delta r_\alpha^2(t)$ obtained from mode-coupling theory with MD-simulated $S(q)$. Solid (dashed) lines: small-particle MSD with (without) interactions between small particles, densities as labeled. Dotted: big-particle MSD for the highest density shown.

acting small particles can channel themselves along favorable paths, not unlike single-file diffusion. The self-part of the small-particle van Hove correlation function, $G_s(r, t) = \langle \delta[\bar{r}_s^s(t) - \bar{r}_s^s(0) - \bar{r}] \rangle$, shown in Fig. 4, agrees with this. $P_s(r, t) = 4\pi r^2 G_s(r, t)$ can be interpreted as the probability density to find a small particle having traveled distance r in time t ; it has a multi-peak structure on the length scale set by the large particles, indicating that small particles move along preferred locations (as known in ion-conducting melts [36]). But for transparent small particles, the peaks are broadened and decay slower, indicating that these particles spend more time in each of the local traps before proceeding to the next preferred location. Note for the interacting small particles, at $t = 239.3$, an additional peak on the length scale σ_{ss} , which is absent without small-particle interactions. This is consistent with assuming an interaction-mediated transport in the former case that is missing in the latter.

No exact results are known for our binary mixture. The MCT double-transition scenario [19–21] is in line with our results. Ignoring potentially dangerous long-wavelength fluctuations [37, 38], we solved the MCT equations of motion with discrete wave numbers $q_i = (i - 1/2)\Delta q \sigma_1^{-1}$ with $i = 1, \dots, 120$, $\Delta q = 0.4$ and additional low- q cutoff $q_0 = 4\sigma_1^{-1}$. MCT then predicts $x_{\text{MCT}} = 1/2$ generically, for both models, and in contrast to the suggested picture above. Making small particles ‘transparent’ enters in MCT only through the $S_{\alpha\beta}(q)$ (taken from MD, cf. inset of Fig. 1).

As Fig. 5 demonstrates, the theory still reproduces some qualitative trends seen in the MD data: (i) while the big-particle MSD exhibits ordinary glassy two-step behavior (localization length around $0.1\sigma_1$), $\delta r_s^2(t)$ shows a different signature in the time windows accessible to the simulation. This is the precursor of the double-transition scenario, where big particles freeze to form a glass at $\rho_c \approx 2.29$, followed by an additional small-particle arrest at a higher density $\rho_c^s > \rho_c$. (ii) At low densities,

transparent-small diffusion (dashed) is faster than the one for interacting small particles (solid lines), as expected from the reduced scattering frequency. This also holds for high densities at intermediate times.

For large t and high ρ , the MCT results show that even a fixed exponent x could give rise to a slowing down in the MSD when switching off small-particle interaction. In the theory, this arises from a shift of $\rho_c^s \approx 2.30$ to a lower $\rho_c^s \approx 2.24$, rendering transport slower at fixed ρ . While this MCT result has the above mentioned caveats, it shows that one has to be careful assigning different ‘universality classes’ (different exponents x) to the two model systems studied in simulation. However, the remarkable finding that transport becomes slower on removing excluded-volume constraints survives even then – translated into a shift of MCT’s critical density to lower ρ upon removing interactions. This arises from subtle changes in $S_{ss}(q)$, beyond the scope of MCT.

Let us summarize the main results. We studied a disparate-size mixture of purely repulsive soft spheres whose dynamics can be understood as the approach to two distinct, purely dynamical arrest transitions: (i) an ordinary glass transition connected with big-particle transport, where small-particle diffusion does not vanish, and (ii) a localization transition for small-particle transport at a higher density. As a precursor, the small-particle mean-squared displacement exhibits power-law anomalous diffusion, $\delta r_s^2(t) \propto t^x$, over increasingly large length scales. This naturally explains an order-of-magnitude decoupling between diffusion coefficients, rendering our binary soft-sphere mixture a minimal model for fast ion transport in amorphous materials.

The anomalous diffusion in our binary mixture is a *many-particle* phenomenon: upon switching off interactions between the small particles, effective power-law exponents appear to decrease. As a consequence, excluded-volume interactions between the small particles *accelerate* their transport in the binary mixture. This is remarkable, since in the high-density regime one usually expects excluded volume to hinder individual particle motion. While a cross-over from single-particle (Lorentz-gas like) dynamics to a many-particle interaction-mediated transport would nicely explain our findings, such a connection remains to be established theoretically.

We acknowledge discussions with T. Franosch and F. Höfling and thoughtful comments by W. Götze. ThV is supported by the Helmholtz-Gemeinschaft (Hochschul-Nachwuchsgruppe VH-NG 406) and the Zukunftskolleg of the Universität Konstanz.

[1] A. K. Jonscher, *Nature (London)* **267**, 673 (1977).

[2] T. J. Feder, I. Brust-Mascher, J. P. Slattery, B. Baird, and W. W. Webb, *Biophys. J.* **70**, 2767 (1996).

- [3] I. Y. Wong, M. L. Gardel, D. R. Reichman, E. R. Weeks, M. T. Valentine, A. R. Bausch, and D. A. Weitz, *Phys. Rev. Lett.* **92**, 178101 (2004).
- [4] D. S. Banks and C. Fradin, *Biophys. J.* **89**, 2960 (2005).
- [5] K. Hahn, J. Kärger, and V. Kukla, *Phys. Rev. Lett.* **76**, 2762 (1996).
- [6] D. S. Sholl and K. A. Fichthorn, *Phys. Rev. Lett.* **79**, 3569 (1997).
- [7] P. A. Netz and T. Dorfmueller, *J. Chem. Phys.* **103**, 9074 (1995).
- [8] S. Babu, J. C. Gimel, and T. Nicolai, *J. Phys. Chem. B* **112**, 743 (2008).
- [9] H. Scher and E. W. Montroll, *Phys. Rev. B* **12**, 2455 (1975).
- [10] Q.-H. Wei, C. Bechinger, and P. Leiderer, *Science* **287**, 625 (2000).
- [11] C. Lutz, M. Kollmann, and C. Bechinger, *Phys. Rev. Lett.* **93**, 026001 (2004).
- [12] B. Lin, M. Meron, B. Cui, S. A. Rice, and H. Diamant, *Phys. Rev. Lett.* **94**, 216001 (2005).
- [13] P. Maass, J. Petersen, A. Bunde, W. Dieterich, and H. Roman, *Phys. Rev. Lett.* **66**, 52 (1991).
- [14] M. J. Saxton, *Biophys. J.* **66**, 394 (1994).
- [15] R. Metzler and J. Klafter, *Phys. Rep.* **339**, 1 (2000).
- [16] T. E. Harris, *J. Appl. Probab.* **2**, 323 (1965).
- [17] D. G. Levitt, *Phys. Rev. A* **8**, 3050 (1973).
- [18] L. Lizana and T. Ambjörnsson, *Phys. Rev. Lett.* **100**, 200601 (2008).
- [19] J. Bosse and J. S. Thakur, *Phys. Rev. Lett.* **59**, 998 (1987).
- [20] J. Bosse and Y. Kaneko, *Phys. Rev. Lett.* **74**, 4023 (1995).
- [21] L. Sjögren, *Phys. Rev. A* **33**, 1254 (1986).
- [22] W. Götze, in *Amorphous and Liquid Materials*, edited by E. Lüscher, G. Fritsch, and G. Jacucci (Nijhoff Publishers, Dordrecht, 1987), NATO ASI Series, pp. 34–81.
- [23] A. Imhof and J. Dhont, *Phys. Rev. Lett.* **75**, 1662 (1995).
- [24] A. Imhof and J. Dhont, *Phys. Rev. E* **52**, 6344 (1995).
- [25] A. Moreno and J. Colmenero, *J. Chem. Phys.* **125**, 164507 (2006).
- [26] Th. Voigtmann and J. Horbach, *Europhys. Lett.* **74**, 459 (2006).
- [27] V. Krakoviack, *Phys. Rev. Lett.* **94**, 065703 (2005).
- [28] V. Krakoviack, *J. Phys.: Condens. Matter* **17**, S3565 (2006).
- [29] J. Kurzidim, D. Coslovich, and G. Kahl (2009), arXiv:0906.0929.
- [30] W. Götze, E. Leutheusser, and S. Yip, *Phys. Rev. A* **23**, 2634 (1981).
- [31] W. Götze, E. Leutheusser, and S. Yip, *Phys. Rev. A* **25**, 533 (1982).
- [32] S. Havlin and D. Ben-Avraham, *Adv. Phys.* **51**, 187 (2002).
- [33] F. Höfling, T. Franosch, and E. Frey, *Phys. Rev. Lett.* **96**, 165901 (2006).
- [34] F. Höfling and T. Franosch, *Phys. Rev. Lett.* **98**, 140601 (2007).
- [35] F. Höfling, T. Munk, E. Frey, and T. Franosch, *J. Chem. Phys.* **128**, 164517 (2008).
- [36] J. Horbach, W. Kob, and K. Binder, *Phys. Rev. Lett.* **88**, 125502 (2002).
- [37] E. Leutheusser, *Phys. Rev. A* **28**, 1762 (1983).
- [38] V. Krakoviack, *Phys. Rev. E* **79**, 061501 (2009).